

The Brightness of VisorSat-Design Starlink Satellites

Anthony Mallama

anthony.mallama@gmail.com

2021 January 2

Abstract

The mean of 430 visual magnitudes of VisorSats adjusted to a distance of 550-km (the operational altitude) is 5.92 ± 0.04 . This is the characteristic brightness of these satellites when observed at zenith. VisorSats average 1.29 magnitudes fainter than the original-design Starlink satellites and, thus, they are 31% as bright.

1. Introduction

The rapidly growing population of bright satellites in low-earth-orbit is beginning to interfere with ground-based astronomy (Otarola et al., 2020, Walker et al., 2020, Tyson et al., 2020, Gallozzi et al., 2020, Hainaut and Williams, 2020 and McDowell, 2020). The SpaceX company has launched hundreds of Starlink communication satellites during the past two years and plans to put thousands more into orbit in the near future. OneWeb is actively pursuing a similar project and other companies may follow.

SpaceX has engaged with the astronomical community to address this issue. As a result they have developed a VisorSat model of Starlink that includes a Sun shade to make the satellites appear dimmer. This paper characterizes the observed brightness of VisorSat-design spacecraft in visible light and compares it to that of the original Starlink design.

Section 2 of this paper defines the magnitudes used herein and discusses the illumination phase angle which can affect brightness. Then Section 3 describes the physical shape of Starlink satellites and discusses their orbits as these factors pertain to brightness. Section 4 describes the sources of satellite

magnitudes used in this study as well as the data processing techniques. Section 5 presents the findings which include the mean VisorSat magnitude, its uncertainty, the dispersion and the phase function. Section 6 compares the brightness of VisorSat with that of the original-design Starlink satellites and with the OneWeb satellite constellation. Section 7 discusses some limitations of this study. Section 8 briefly addresses VisorSats below the operational altitude as well as brightness surges. Section 9 gives the conclusions.

This study is part of the author's work with the Satellite Observations Working Group (Otarola et al., 2020). Most of the SOWG members record observations made through spectral filters. The visual magnitude results in this paper characterize satellite brightness across all visible wavelengths and complement the color-filtered photometry being carried out by other members of the SOWG.

2. Magnitudes and phase angles

Visual magnitudes represent satellite brightness in combined blue, green and red light with an effective wavelength in green. The band-pass sensitivity is centered near 0.6 micron and its width is about 0.4 micron. Visual magnitudes are a close match to the V-band of the Johnson-Cousins photometric system although the bandwidth of V is narrower.

The *apparent magnitude* is that recorded by a sensor after correction for atmospheric extinction. An analogy to the absolute magnitude of astronomers is the *1000-km magnitude* used by the satellite community. The 1000-km magnitude is an adjustment of apparent brightness to that standard distance which allows for comparisons between multiple satellite constellations at different altitudes.

Finally, there is a *standard magnitude* that is intended to account for the illumination phase angle which is measured at the satellite between the Sun and the observer. In principle the standard magnitude gives the brightness of a half-illuminated satellite at 1000 km distance. The adjustment between the 1000-km magnitude and the standard magnitude is given in Equation 1,

$$C = 2.5 * \log_{10} (0.5 + 0.5 \cos B) + 0.753$$

Equation 1

where C is the correction to be added. For an observer at phase angle B the term inside the parentheses represents the fraction of a spherical object that is illuminated by the Sun. The value 0.753 sets the correction to zero for a satellite at $B = 90^\circ$. In practice the standard magnitude is of limited value for Starlink satellites because they are not shaped like spheres.

A potentially useful approach for Starlink is to derive an empirical phase function by determining a least-squares fit between the 1000-km magnitudes and their phase angles. An empirical fit for VisorSat magnitudes is presented later in this paper.

The SOWG generally employs the Minnaert (1941) bidirectional reflectance function to process observed magnitudes. Other formalisms can be used, too. Cole (2020) developed a physical model for VisorSats that includes its solar array.

3. Starlink satellites and their orbits

The orbital characteristics of Starlink satellites along with their physical size, shape, attitude (that is, their orientation in space) and reflective properties determine their brightness. Spacing between the observer and the satellite affects brightness according to the inverse square of the distance. SpaceX plans to distribute Starlink satellites into several orbital 'shells' of different altitudes and, thus, different distances. To date all satellites have been assigned to the 550 km altitude shell.

Starlink satellites are launched in batches of about 60 at a time on a single rocket. They are initially injected into lower altitude orbits where they reside until precession advances them to the desired celestial plane. Then they ascend to their final orbital altitude in groups of about 20 where they are spaced apart by 5 minutes of time and orbit the Earth in 95 minutes. These groups of 20 may be observed from one location on a single night.

The satellites themselves consist of a flat-panel shaped bus and a large attached solar array. The flat panel is nominally oriented perpendicular to the nadir direction and the solar panel is positioned to intercept sunlight. The bus appears to have both diffusive and specularly reflective surfaces.

Starlink-1436 was the first VisorSat-design satellite to be launched. In this model a Sun shade was added to the bus in order to reduce the amount of sunlight reflected from the nadir side toward observers on the Earth's surface. That initial VisorSat was orbited on 2020 June 4 on the seventh operational Starlink launch designated L7. Beginning with the L9 launch of 2020 August 7 all Starlink satellites have been VisorSats.

4. Observation and data processing

The magnitudes analyzed in this paper are visual as defined in Section 2. That is, they represent the brightness of Starlink satellites in combined red, green and blue colors with an effective wavelength near 0.6 micron.

The data come from three sources. Two of them are experienced visual observers using binoculars. J. Respler records satellite magnitudes from coordinates 40° north and 74° west while the author observes from 39° north and 77° west. Satellite brightness is determined by comparison with nearby stars of known magnitudes using interpolation. The observers aim to achieve magnitudes that are accurate to about 0.2 magnitudes. Each apparent magnitude is converted to a 1000-km magnitude based on the satellite range at the time of observation. An associated phase angle is determined from the positions of the satellite, Sun and observer.

On 7 occasions out of 290 binocular observations the satellite was too faint to be seen. Since the limiting magnitude is usually about 8 and few satellites are close to that limit, the value 8.5 was assigned for those 7 observations. Figure 1 illustrates the distribution of apparent magnitudes.

The third source of data is the Mini-MegaTORTORA (MMT) automated observatory (Karpov et al. 2015) in Russia at 44° north and 41° east. Each of the 9 MMT channels consists of a 71 mm diameter f/1.2 lens and a 2160 x 2560 sCMOS detector. Unfiltered MMT magnitudes are within 0.1 magnitude of the Johnson-Cousins V band-pass for objects with small B-V color indices according to a color transformation formula kindly provided by S. Karpov (private communication). Mallama (2020a) found MMT magnitudes to be consistent with those of visual observers.

The online MMT database lists standard magnitudes which include the phase angle correction for a spherical body described in Section 2. Since Starlink satellites are not spherical the correction indicated

by Equation 1 is removed in order to give the 1000-km magnitude for the purpose of this study. When a satellite is recorded simultaneously by two separate MMT channels the magnitudes may differ by 0.1 - 0.2 magnitude which suggests that accuracy is of that order.

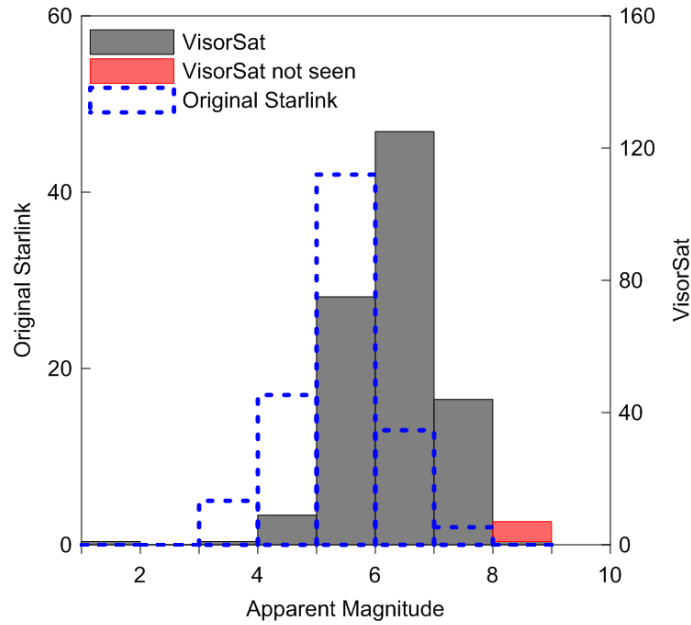


Figure 1. Histogram of apparent VisorSat magnitudes recorded by the visual observers. Also shown are the assigned magnitudes where the satellites were too faint to be seen, along with apparent magnitudes for original-design Starlink satellites.

Starlink satellites spend the great majority of their lifetime in orbit at the 550 km operational altitude. Furthermore, SpaceX (2020) indicates that they adjust the configuration of the solar panel differently during the ascent and the operational phases. Therefore, only observations of satellites at the operational altitude were selected for the analysis in the next section, while observations of satellites at lower altitudes are addressed later. Measurements taken when the satellite was in the Earth's penumbral shadow were not used. Each of the 430 observations used in Section 5 sampled a different satellite pass. The data are listed in the Appendix A.

5. Brightness characterization

The mean 1000-km magnitude for satellites at the 550 km operational altitude is 7.22 ± 0.04 and the standard deviation of the individual magnitudes is 0.85. The median magnitude is somewhat fainter at 7.36 indicating that the mean is skewed by a few very bright observations. The mean adjusted to a range of 550 km gives magnitude 5.92 which is an indication of VisorSat brightness at zenith.

Figure 2 shows the magnitudes plotted as a function of phase angle. The linear and quadratic fits indicate that the satellites are brighter at small phase angles as expected. However, the standard deviation remains at 0.085 after the linear fit is applied and it only reduces to 0.084 for the quadratic fit. So phase functions are of little practical value in predicting satellite brightness. The best fitting equations are given in Table 1.

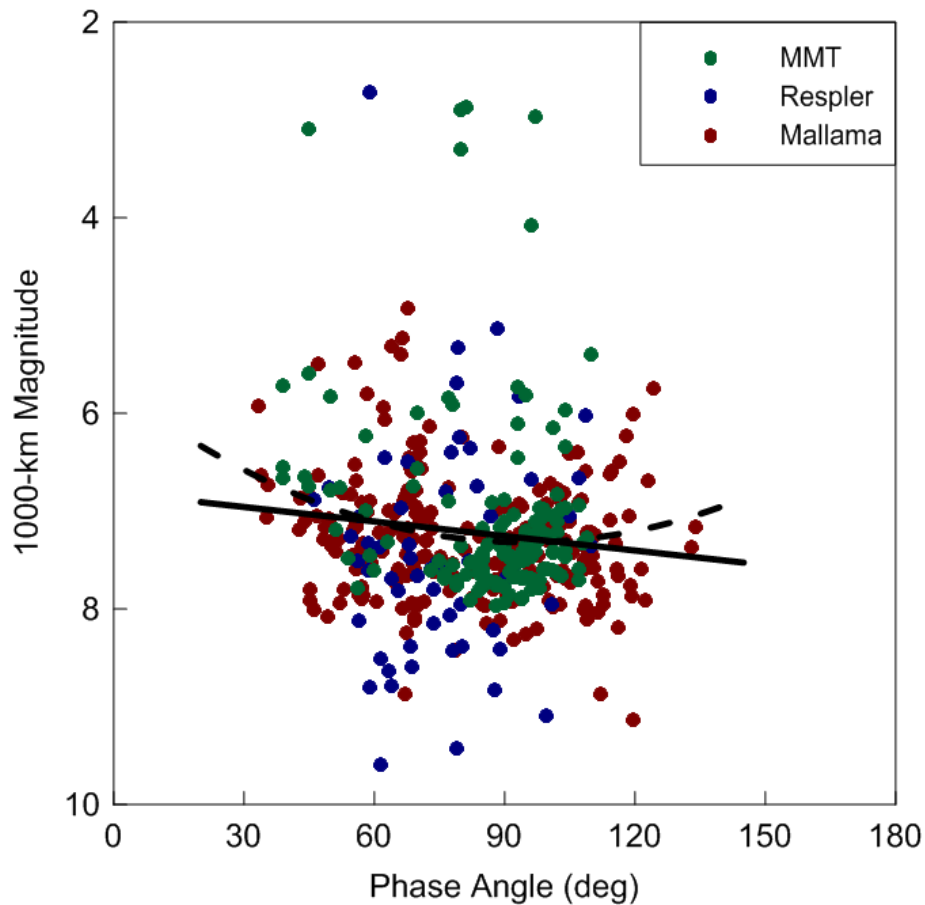


Figure 2. The phase function with linear and quadratic least-squares fits.

Observations of original-design Starlink satellites also evidenced large observed scatter with little reduction from modeling. Otarola et al. (2020) determined a standard deviations of 0.75 magnitude for POMENIS V-band photometry of satellites above 550 km before normalization techniques were applied and that only reduced to 0.69 afterward. Likewise, Mallama (2020a) derived 0.67 for 1000-km original-design Starlink magnitudes and 0.65 after a linear phase angle correction was applied.

Table 1. Phase Functions

Linear $M_v = 6.809 + 0.00495 * P$

Quadratic $M_v = 5.732 + 0.03352 * P - 0.000177 * P^2$

M_v = visual magnitude

P = phase angle in degrees

The large dispersion values are expected. Visual observers have often noticed that Starlink satellites viewed in succession with nearly identical satellite-Sun-observer geometries can vary widely in brightness. For example, J. Respler wrote “there were 4 pairs [of satellites] with second following first by several seconds. In each case the first was mag 4-6. The second was 2-3 mags brighter” (<http://www.satobs.org/seesat/Mar-2020/0126.html>).

Additionally, MMT light curves demonstrate substantial and seemingly erratic magnitude changes as illustrated in Figure 3. The large brightness variations seen by visual observers and recorded by MMT are probably due to satellite attitudes. Thus, accurate prediction of the brightness of any given satellite at any given time may remain a difficult problem to solve.

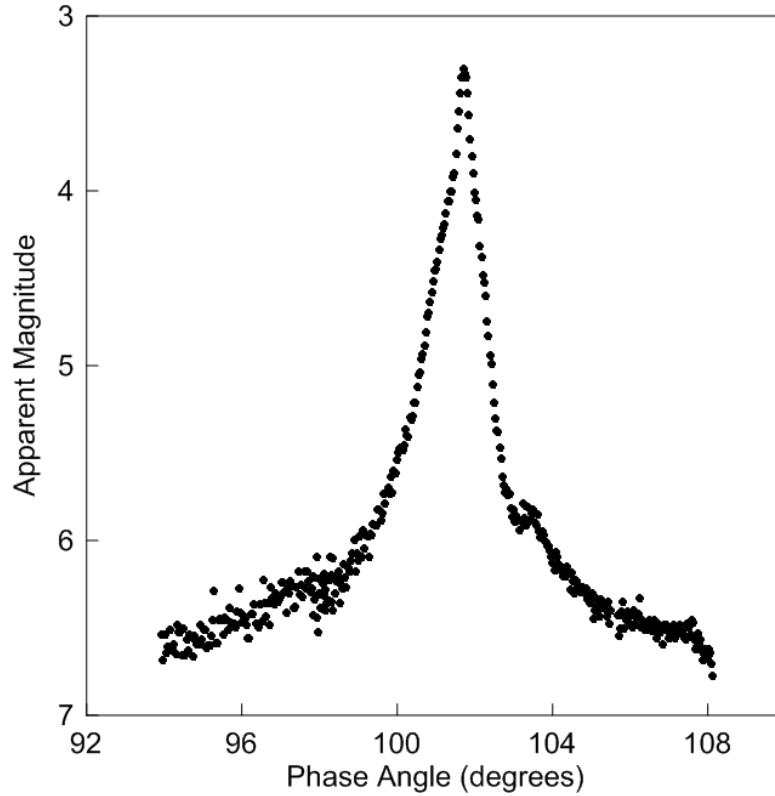


Figure 3. MMT light curve of Starlink-1549 recorded on 2020 November 27. The large brightness surge is not explained by the phase angles of the observations.

Two other independent variables besides phase angle have been examined. Figure 4 shows magnitudes plotted versus calendar days. Meanwhile, Figure 5 shows magnitudes versus days elapsed since a satellite reached the 550 km operational altitude. Both of these functions seem to indicate dimming over time and these effects may be aliasing. The best fit to the calendar day plot indicates a fading of 0.52 magnitude between day 236 and 363 of calendar year 2020. The power law fitted to the magnitudes in Figure 5 suggests about half a magnitude of fading shortly after the satellites attain 550 km altitude.

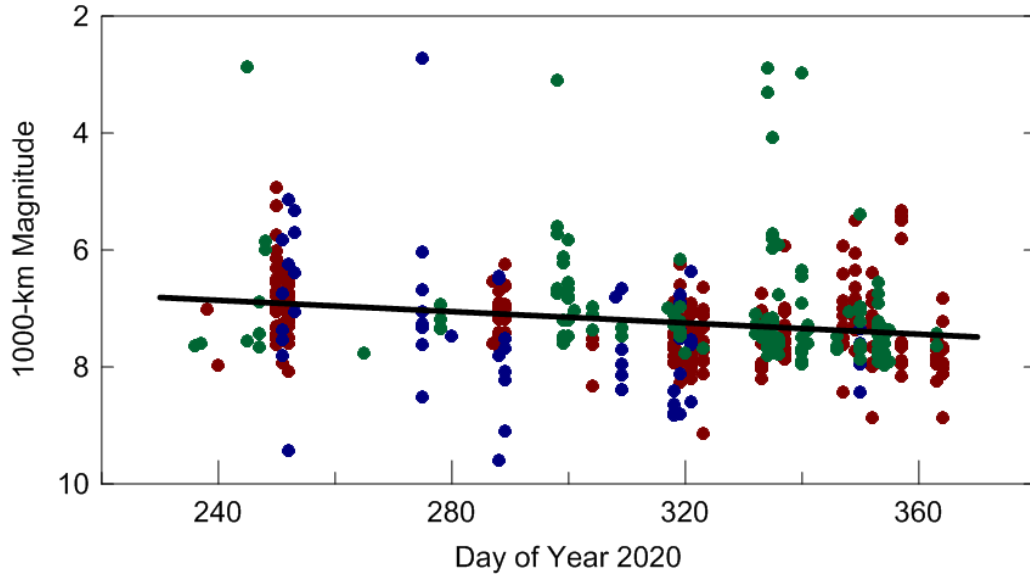


Figure 4. Brightness as a function of time.

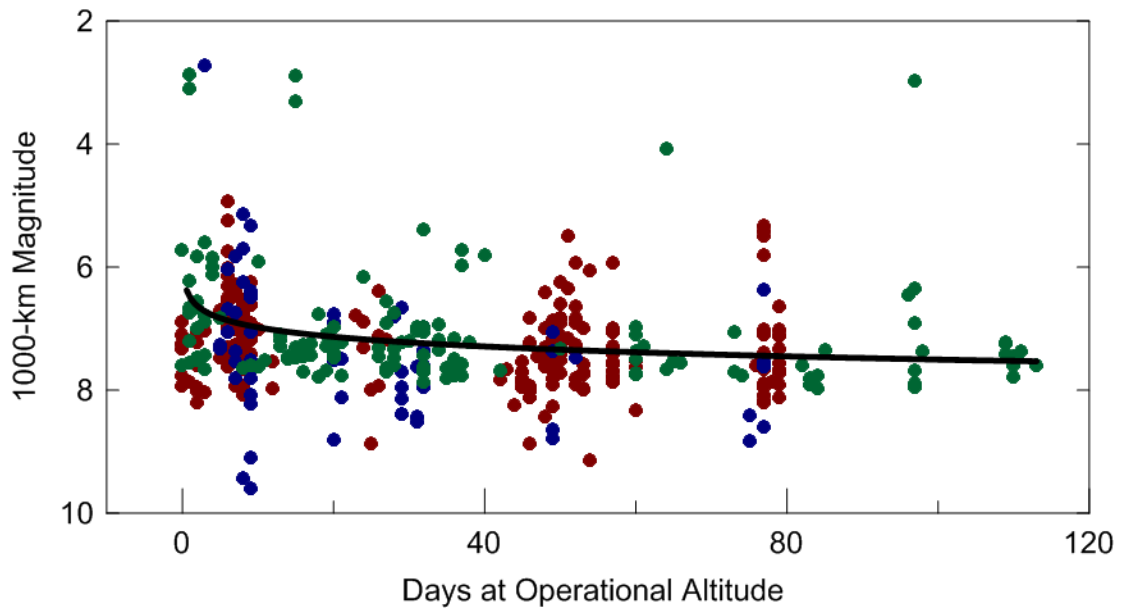


Figure 5. Brightness versus time after reaching 550 km altitude fitted with a power law.

6. Comparison with original-design Starlink and with OneWeb

There are several hundred original-design Starlink satellites in orbit. The mean VisorSat magnitude reported in the previous section is 1.29 fainter than that of the original-design satellites as reported by Mallama (2020a). Thus, VisorSats average 31% as bright as their predecessors.

OneWeb satellites are another constellation being launched in great numbers. These spacecraft have large solar arrays on long support arms and dish-like antennas on shorter arms. Their operational altitude of 1,200 km is more than twice that of Starlink. Mallama (2020b) determined a mean 1000-km magnitude of 7.18 +/-0.03 for OneWeb based on MMT observations. An analysis of visual binocular observations which were reported at a later time (satobs.org/seesat/Dec-2020/0072.html) gave results that are consistent with those from MMT. The 1000-km value adjusted to the nominal 1,200 km altitude of a OneWeb satellite in orbit corresponds to magnitude 7.58. Thus, VisorSats satellites are approximately the same brightness as OneWeb at a common distance but they are much brighter than OneWeb at their respective operational altitudes. Table 2 summarizes these comparisons.

Table 2. Magnitude comparisons

Satellite	1000-km	Operational Altitude	Uncertainty
VisorSat	7.22	5.92	+/-0.04
Original Starlink	5.93	4.63	+/-0.02
OneWeb	7.18	7.58	+/-0.03

7. Limitations of this study

Several factors place limits on the accuracy and the general applicability of the results in this paper. First is the geographic distribution of the three data sources noted in Section 3. The MMT is located in Russia and the two visual observers are located in the eastern United States. If spacecraft attitude is being adjusted geographically for operational reasons then the results presented here may not be representative of other regions. Furthermore, the Sun's varying declination throughout the year may

affect satellite brightness in a complicated way that depends on a combination of season and geographic location.

Another limiting factor is the short time span of the observations which begins in 2020 August and ends in December. Since spacecraft attitude can be actively controlled, the observed magnitudes during this period may not reflect those at later times.

Lastly, the MMT standard magnitudes and phase angles used in the analysis are averages of those for each satellite track. The magnitudes were copied from the MMT database while the phase angles were estimated by eye from track plots. The estimated phase angles are accurate to about 1 degree. A more rigorous (and time consuming) approach would be to associate every magnitude in every track with its corresponding phase angle.

8. Lower altitude observations and flaring

Besides the data already discussed the author measured 22 magnitudes of VisorSats that were below the operational altitude. The mean 1000-km magnitude was 7.54 ± 0.03 and the mean altitude was 417 km. Thus, the satellites were not especially bright in an absolute sense although their mean apparent brightness was rather high at magnitude 5.65. The observations are listed in Appendix B.

The original Starlink satellites were observed to flare in brightness by up to 10 magnitudes on several occasions in 2020 April (Mallama 2020a). These reports were posted on the SeeSat-L mailing list at <http://www.satobs.org>. However, there have been no further reports of extreme flaring events for original or VisorSat Starlink satellites since that time.

9. Conclusions

Magnitudes of VisorSat satellites at their 550 km altitude measured by the MMT automated observatory in Russia and by two visual observers in the United States are analyzed. The main conclusion is that the mean of 430 visual magnitudes adjusted to a 550 km range is 5.92 ± 0.04 . This is their characteristic brightness when seen at zenith. VisorSats average 1.29 magnitudes fainter than the original-design Starlink satellites. Thus, VisorSats are 31% as bright as their predecessors.

The following findings are also discussed. There is some indication of a modest brightness decline after the first few days of a satellite at 550 km and there may have been a general dimming over time in year 2020. Satellites below the operational altitude are not especially bright in an absolute sense but their apparent brightness is high. No extremely bright flaring of VisorSats has been reported since 2020 April.

References

- Cole, R.E. 2020. A sky brightness model for the Starlink "Visorsat" spacecraft. Research Note of the AAS. <https://iopscience.iop.org/article/10.3847/2515-5172/abc0e9>.
- Gallozzi, S., Scardia, M., and Maris, M. 2020. Concerns about ground based astronomical observations: a step to safeguard the astronomical sky. <https://arxiv.org/pdf/2001.10952.pdf>.
- Hainaut, O.R., and Williams, A.P. 2020. Impact of satellite constellations on astronomical observations with ESO telescopes in the visible and infrared domains. *Astron. Astrophys.* manuscript no. SatConst. <https://arxiv.org/abs/2003.019pdf>.
- Karpov, S., Katkova, E., Beskin, G., Biryukov, A., Bondar, S., Davydov, E., Perkov, A. and Sasyuk, V. 2015. Massive photometry of low-altitude artificial satellites on minimegaTORTORA. Fourth Workshop on Robotic Autonomous Observatories. RevMexAA.
- Mallama, A. 2020a. Starlink satellite brightness before VisorSat. <https://arxiv.org/abs/2006.08422>.
- Mallama, A. 2020b. The brightness of OneWeb satellites. <https://arxiv.org/abs/2012.05100>.
- Minnaert, M. 1941. The reciprocity principle in lunar photometry. *The Astrophysical Journal*, 93 403. 10.1086/144279.
- McDowell, J. 2020. The low Earth orbit satellite population and impacts of the SpaceX Starlink constellation. *ApJ Let*, 892, L36 and <https://arxiv.org/abs/2003.07446>.
- Otarola, A. (chairman) and Allen, L., Pearce, E., Krantz, H.R., Storrie-Lombardi, L., Tregloan-Reed, J, Unda-Sanzana, E., Walker, C. and Zamora, O. 2020. Draft Report of the Satellite Observations Working Group commissioned by the United Nations, Spain and the International Astronomical Union as the Workshop on Dark and Quiet Skies for Science and Society. <https://owncloud.iac.es/index.php/s/WcdR7Z8GeqfRWxG#pdfviewer>.
- SpaceX 2020. Starlink Discussion National Academy of Sciences April 28, 2020. <https://www.spacex.com/updates/starlink-update-04-28-2020/>
- Tregloan-Reed, J, Otarola, A., Ortiz, E., Molina, V., Anais, J., Gonzalez, R., Colque, J.P. and Unda-Sanza, E. 2020. First observations and magnitude measurement of SpaceX's Darksat. *Astron. Astrophys.*, manuscript no. Darksat_Letter_arXiv_submission_V2. <https://arxiv.org/pdf/2003.07251.pdf>.

Tyson, J.A., Ivezić, Ž., Bradshaw, A., Rawls, M.L., Xin, B., Yoachim, P., Parejko, J., Greene, J., Sholl, M., Abbott, T.M.C., and Polin, D. (2020). Mitigation of LEO satellite brightness and trail effects on the Rubin Observatory LSST. arXiv e-prints, arXiv:2006.12417.

Walker, C., Hall, J., Allen, L., Green, R., Seitzer, P., Tyson, T., Bauer, A., Krafton, K., Lowenthal, J., Parriott, J., Puxley, P., Abbott, T., Bakos, G., Barentine, J., Bassa, C., Blakeslee, J., Bradshaw, A., Cooke, J., Devost, D., Galadí-Enríquez, D., Haase, F., Hainaut, O., Heathcote, S., Jah, M., Krantz, H., Kucharski, D., McDowell, J., Ioan-Reed, J., Wainscoat, R., Williams, A., and Yoachim, P. (2020). Impact of satellite constellations on optical astronomy and recommendations toward mitigations. Bulletin of the Astronomical Society, 52(2), 0206. 10.3847/25c2cfcb.346793b8.

Appendix A.

Summary of 550 km magnitudes

'Cal. Day' is the day number of year 2020.

'Ops. Days' is the time since attaining the 550km operational altitude.

Red entries indicate 'not seen' where apparent magnitude is assigned as 8.5

Starlink Sat #	Cal. Day	Ops. Days	Phase Angle	1000-km Magnitude	Source
1436	238	10	71	7.02	Mallama
1436	240	12	86	7.96	"
1581	250	5	75	7.47	"
1526	250	6	75	7.52	"
1584	250	6	74	7.61	"
1523	250	6	73	7.01	"
1576	250	6	73	6.13	"
1580	250	6	72	7.45	"
1591	250	6	71	6.56	"
1534	250	6	69	6.79	"
1544	250	6	69	6.31	"
1565	250	6	68	4.93	"
1560	250	6	67	5.23	"
1556	250	6	94	6.95	"
1557	250	6	100	7.06	"
1567	250	6	94	7.31	"
1558	250	6	104	7.31	"
1569	250	6	106	7.42	"
1555	250	6	116	6.49	"
1582	250	6	120	6.01	"
1522	250	6	124	5.75	"
1581	250	5	123	6.69	"
1584	251	7	70	6.29	"

1523	251	7	70	6.39	"
1576	251	7	70	7.02	"
1580	251	7	69	7.93	"
1591	251	7	68	6.45	"
1534	251	7	67	6.85	"
1544	251	7	67	7.26	"
1565	251	7	67	7.44	"
1560	251	7	68	6.78	"
1556	251	7	77	6.75	"
1557	251	7	91	7.27	"
1567	251	7	95	7.45	"
1522	252	8	69	7.59	"
1581	252	7	69	6.48	"
1526	252	8	68	6.55	"
1584	252	8	68	6.86	"
1523	252	8	68	7.17	"
1576	252	8	69	6.59	"
1580	252	8	69	8.07	"
1591	252	8	69	6.95	"
1534	252	8	70	7.09	"
1544	252	8	72	7.30	"
1565	252	8	73	7.17	"
1560	252	8	75	7.50	"
1556	252	8	102	6.78	"
1557	252	8	100	6.72	"
1567	252	8	109	7.21	"
1611	287	8	56	7.59	"
1641	287	8	56	6.53	"
1597	288	8	55	7.45	"
1615	288	8	55	7.18	"
1629	288	8	56	6.69	"
1608	288	8	57	7.40	"
1628	288	8	69	7.65	"
1592	288	8	81	7.40	"
1626	288	8	93	6.93	"
1601	288	8	96	7.43	"
1630	288	8	103	6.95	"
1595	288	9	56	7.16	"
1640	288	9	56	7.58	"
1611	288	9	57	6.91	"
1641	288	9	58	7.01	"
1597	288	9	59	6.90	"
1615	289	9	62	7.41	"
1629	289	9	102	7.16	"
1608	289	9	95	7.17	"

1628	289	9	100	6.93	"
1592	289	9	90	6.95	"
1626	289	9	92	6.99	"
1601	289	9	115	6.59	"
1630	289	9	118	6.23	"
1613	289	9	114	6.61	"
1567	304	60	92	8.32	"
1558	304	60	94	7.51	"
1569	304	60	96	7.61	"
1542	318	0	92	7.93	"
1551	318	0	108	6.88	"
1568	318	0	111	7.25	"
1559	318	0	114	7.09	"
1542	319	1	113	7.86	"
1578	319	0	116	7.32	"
1536	319	0	119	7.76	"
1530	318	49	72	7.05	"
1527	318	49	71	7.46	"
1624	318	49	48	7.28	"
1577	318	49	51	7.41	"
1574	318	49	53	7.80	"
1554	318	49	57	7.90	"
1541	318	49	79	7.69	"
1543	318	49	99	7.59	"
1535	318	49	102	7.66	"
1548	319	49	95	8.25	"
1540	319	46	103	7.95	"
1570	319	49	49	7.16	"
1514	319	50	50	7.31	"
1530	319	50	55	6.83	"
1527	319	50	58	7.33	"
1524	319	50	61	7.22	"
1577	319	50	45	6.83	"
1574	319	50	59	7.52	"
1554	319	50	57	7.39	"
1541	319	50	80	6.24	"
1543	319	50	106	7.38	"
1535	319	50	109	6.59	"
1548	319	50	94	7.41	"
1540	320	47	98	7.45	"
1561	320	49	101	7.19	"
1562	320	49	110	7.21	"
1573	321	52	45	7.91	"
1564	321	52	45	7.79	"
1572	321	52	50	7.36	"

1570	321	52	67	6.90	"
1514	321	53	65	6.99	"
1556	321	77	49	8.08	"
1530	321	53	104	7.69	"
1527	321	53	110	7.58	"
1524	321	53	101	7.97	"
1577	321	53	105	7.73	"
1574	321	53	109	7.99	"
1582	321	77	49	7.08	"
1522	321	77	65	7.02	"
1581	321	76	66	7.59	"
1526	321	77	105	7.11	"
1584	321	77	109	7.39	"
1523	321	77	95	7.43	"
1576	321	77	98	8.21	"
1580	322	77	108	7.59	"
1591	322	77	110	7.45	"
1565	323	79	47	6.63	"
1560	323	79	50	7.09	"
1556	323	79	65	7.01	"
1557	323	79	92	7.33	"
1567	323	79	105	7.67	"
1558	323	79	109	8.11	"
1569	323	79	99	7.11	"
1555	323	79	109	7.56	"
1582	323	79	112	7.72	"
1522	323	79	116	7.66	"
1581	323	78	119	7.87	"
1526	323	79	122	7.91	"
1663	333	2	93	7.23	"
1678	333	3	112	8.03	"
1696	333	3	104	7.03	"
1659	333	2	108	8.01	"
1676	333	2	113	7.95	"
1644	333	2	116	8.19	"
1698	333	2	119	7.05	"
1672	333	2	122	7.59	"
1633	333	7	36	6.73	"
1616	333	7	69	7.28	"
1636	333	8	52	7.93	"
1631	337	12	69	7.53	"
1593	337	57	52	7.29	"
1618	337	57	57	7.86	"
1590	337	57	35	7.06	"
1588	337	57	63	6.99	"

1595	337	57	33	5.92	"
1640	337	57	47	7.05	"
1611	337	57	78	7.54	"
1641	337	57	78	7.67	"
1597	337	57	56	7.86	"
1615	337	57	57	7.77	"
1629	337	57	99	7.01	"
1608	337	57	90	7.57	"
1628	337	57	96	7.41	"
1592	337	57	99	7.78	"
1771	347	52	62	5.93	"
1752	347	50	44	7.11	"
1617	347	48	72	7.30	"
1654	347	49	43	6.87	"
1690	347	48	88	6.99	"
1727	347	48	82	7.62	"
1689	347	48	108	7.49	"
1661	347	48	79	8.43	"
1719	347	48	105	6.41	"
1762	347	48	103	7.61	"
1723	349	52	34	6.63	"
1673	349	51	47	5.49	"
1656	349	52	84	7.26	"
1770	349	51	89	6.35	"
1771	349	54	62	6.06	"
1752	349	52	104	6.81	"
1617	349	50	107	6.91	"
1654	349	51	134	7.17	"
1690	349	50	133	7.37	"
1727	349	50	65	7.73	"
1586	352	25	66	7.99	"
1631	352	27	67	7.66	"
1625	352	26	43	7.18	"
1602	352	26	56	7.11	"
1633	352	26	61	7.92	"
1616	352	26	64	7.21	"
1636	352	27	81	7.17	"
1621	352	24	100	7.31	"
1635	352	26	107	6.39	"
1620	352	24	103	6.88	"
1607	352	23	98	6.78	"
1593	357	77	56	5.48	"
1618	357	77	58	5.79	"
1590	357	77	64	5.32	"
1588	357	77	66	5.40	"

1595	357	77	83	7.89	"
1640	357	77	86	8.15	"
1611	357	77	100	7.91	"
1641	357	77	103	7.66	"
1597	357	77	109	7.96	"
1615	357	77	110	7.58	"
1629	357	77	116	7.59	"
1538	363	45	70	7.95	"
1525	363	44	67	8.25	"
1529	363	42	77	7.81	"
1571	363	45	85	7.95	"
1552	363	45	88	7.53	"
1579	363	45	87	7.81	"
1532	363	45	89	7.69	"
1539	363	45	91	7.86	"
1551	364	46	46	8.01	"
1568	364	46	53	6.81	"
1559	364	46	71	7.93	"
1515	364	46	69	8.12	"
1538	364	46	89	8.11	"
1525	364	45	88	7.71	"
1529	364	43	90	7.65	"
1571	364	46	67	7.21	"
1514	323	54	119	9.13	"
1598	352	25	67	8.87	"
1552	364	46	112	8.87	"
1523	251	7	74	7.53	Respler
1580	251	7	66	7.81	"
1534	251	7	61	7.37	"
1560	251	7	84	6.75	"
1556	251	7	93	5.83	"
1591	252	8	80	6.24	"
1544	252	8	88	5.13	"
1581	253	8	79	5.69	"
1526	253	9	78	6.40	"
1584	253	9	87	7.05	"
1576	253	9	79	5.33	"
1554	275	6	109	6.03	"
1541	275	6	96	6.67	"
1540	275	3	59	2.72	"
1561	275	5	59	7.33	"
1564	275	5	54	7.26	"
1565	275	31	59	7.61	"
1514	275	6	57	7.05	"
1557	275	31	62	8.51	"

1436	280	52	68	7.48	"
1611	288	9	62	6.45	"
1641	288	9	68	6.49	"
1597	288	9	74	7.79	"
1615	289	9	77	8.07	"
1629	289	9	82	7.51	"
1608	289	9	87	8.22	"
1628	289	9	85	7.51	"
1592	289	9	90	7.68	"
1595	308	28	76	6.79	"
1601	309	29	107	6.66	"
1630	309	29	101	7.96	"
1619	309	29	80	8.39	"
1634	309	29	74	8.15	"
1593	309	29	68	8.39	"
1618	309	29	64	7.69	"
1524	318	49	63	8.64	"
1577	318	49	64	8.79	"
1582	318	75	89	8.41	"
1535	318	49	105	7.05	"
1548	319	49	110	7.36	"
1657	319	21	92	7.49	"
1752	319	20	59	8.80	"
1654	319	21	56	8.11	"
1690	319	20	56	7.51	"
1727	319	20	46	6.88	"
1661	319	20	50	6.76	"
1567	321	77	69	8.59	"
1558	321	77	75	7.59	"
1569	321	77	82	6.36	"
1555	321	77	84	7.62	"
1522	321	77	93	7.53	"
1538	350	32	80	7.95	"
1525	350	31	78	8.43	"
1552	350	32	73	7.59	"
1579	350	32	68	7.34	"
1532	350	32	70	7.66	"
1539	350	32	66	6.97	"
1565	252	8	79	9.43	"
1595	288	9	61	9.59	"
1601	289	9	100	9.09	"
1522	318	75	88	8.83	"
1436	236	8	76	7.64	MMT
1436	237	9	60	7.60	"
1436	265	37	88	7.75	"

1436	278	50	108	7.32	"
1436	341	113	107	7.59	"
1556	245	1	84	7.56	"
1556	248	4	77	5.84	"
1557	247	3	81	7.65	"
1557	248	4	70	6.00	"
1558	247	3	90	6.89	"
1565	245	1	81	2.87	"
1567	247	3	85	7.43	"
1534	278	34	107	6.94	"
1544	278	34	98	7.17	"
1565	278	34	95	7.34	"
1771	298	3	45	5.59	"
1771	299	4	93	6.11	"
1656	298	1	45	3.09	"
1723	298	1	39	6.66	"
1723	299	2	54	7.48	"
1752	298	1	45	6.74	"
1752	299	2	94	7.51	"
1657	299	1	51	7.19	"
1673	298	0	39	5.72	"
1673	299	1	58	6.23	"
1617	299	0	99	7.59	"
1767	300	2	39	6.56	"
1523	304	60	89	7.36	"
1576	304	60	90	7.10	"
1591	304	60	104	6.97	"
1562	301	31	92	7.04	"
1583	300	30	95	7.20	"
1514	336	66	78	7.55	"
1570	336	65	82	7.53	"
1572	335	64	96	4.08	"
1573	335	64	103	7.67	"
1515	334	16	96	7.33	"
1525	335	16	96	7.27	"
1529	334	13	85	7.18	"
1529	335	14	94	7.45	"
1532	336	18	52	6.76	"
1533	317	2	58	6.99	"
1533	332	17	94	7.43	"
1533	334	19	76	7.68	"
1538	334	16	90	7.44	"
1538	335	17	100	7.25	"
1539	333	15	88	7.30	"
1549	332	13	102	7.10	"

1549	333	14	84	7.49	"
1552	336	18	56	7.79	"
1563	334	15	80	3.31	"
1566	332	13	98	7.28	"
1566	334	15	80	2.90	"
1588	309	28	97	7.32	"
1608	323	42	92	7.68	"
1640	309	28	85	7.47	"
1656	335	38	98	7.21	"
1654	319	21	102	7.21	"
1654	335	37	92	7.57	"
1657	300	2	44	6.65	"
1673	300	2	50	5.82	"
1673	335	37	104	5.97	"
1617	319	20	104	7.39	"
1617	335	36	90	7.77	"
1661	319	20	93	7.48	"
1661	334	35	84	7.63	"
1665	319	20	95	7.45	"
1665	335	36	94	7.69	"
1689	319	20	95	7.25	"
1689	334	35	84	7.81	"
1690	319	20	99	6.97	"
1690	335	36	89	7.16	"
1771	300	5	102	6.82	"
1771	319	24	101	6.15	"
1771	335	40	95	5.81	"
1723	300	3	50	6.79	"
1752	300	2	104	7.47	"
1770	335	37	93	5.73	"
1719	318	19	97	7.10	"
1719	319	20	90	7.42	"
1721	319	20	91	7.45	"
1727	319	20	97	7.41	"
1727	320	21	79	7.76	"
1762	318	19	90	7.29	"
1762	335	36	95	7.49	"
1526	340	97	87	6.90	"
1526	341	98	90	7.37	"
1534	340	97	95	7.67	"
1544	340	97	94	7.88	"
1565	340	97	90	7.94	"
1582	340	97	104	6.34	"
1591	340	97	97	2.97	"
1581	340	96	93	6.45	"

1549	346	27	102	7.63	"
1588	340	60	88	7.73	"
1590	340	60	79	7.71	"
1595	340	60	85	7.49	"
1597	341	61	109	7.28	"
1640	340	60	85	7.74	"
1631	336	11	75	7.51	"
1602	336	10	78	5.91	"
1625	336	10	73	7.61	"
1696	346	16	107	7.71	"
1663	346	15	91	7.48	"
1556	353	109	98	7.21	"
1556	354	110	98	7.79	"
1558	355	111	80	7.36	"
1560	353	109	99	7.23	"
1560	354	110	100	7.60	"
1565	353	109	101	7.41	"
1565	354	110	96	7.46	"
1548	354	85	86	7.34	"
1562	353	83	94	7.90	"
1562	354	84	88	7.96	"
1564	353	83	96	7.80	"
1564	354	84	89	7.76	"
1540	354	82	85	7.59	"
1540	355	83	82	7.91	"
1515	350	32	103	6.98	"
1532	350	32	91	7.86	"
1538	350	32	110	5.39	"
1539	350	32	86	7.70	"
1552	350	32	94	7.68	"
1559	350	32	101	7.05	"
1571	350	32	98	7.70	"
1579	350	32	91	7.62	"
1525	350	31	98	6.96	"
1529	350	29	98	7.21	"
1608	353	73	96	7.70	"
1615	353	74	85	7.77	"
1631	353	28	69	6.74	"
1636	353	28	101	7.60	"
1602	353	27	77	6.90	"
1616	353	27	96	7.69	"
1625	353	27	70	6.56	"
1586	353	26	63	7.31	"
1598	353	26	59	7.45	"
1665	348	73	99	7.05	"

1663	363	32	101	7.43	"
1700	363	32	85	7.64	"

Appendix B.

Summary of magnitudes below 550 km

'Cal. Day' is the day number of year 2020.

'Ops. Days' (negative) is the time since attaining the 550km operational altitude.

Starlink Sat #	Cal Day	Ops. Days	Phase Angle	1000-km Magnitude	Source	Altitude km
1569	231	-13	193	7.60	Mallama	457
1555	231	-13	193	7.69	"	458
1591	231	-13	193	7.79	"	458
1534	231	-13	193	8.37	"	458
1571	232	-85	265	7.80	"	380
1577	232	-36	216	7.40	"	380
1552	232	-36	216	7.21	"	380
1574	232	-36	216	7.42	"	380
1579	232	-85	265	7.22	"	380
1554	232	-36	216	7.02	"	380
1532	232	-85	265	7.23	"	380
1541	232	-36	216	7.03	"	380
1539	232	-85	265	7.24	"	380
1543	232	-36	216	7.04	"	380
1549	232	-86	266	7.04	"	380
1535	232	-36	216	7.45	"	380
1548	232	-36	216	6.86	"	380
1533	232	-1	181	7.07	"	380
1540	232	-46	226	6.86	"	380
1563	318	-1	181	9.36	"	549
1578	318	-1	181	8.66	"	549
1536	318	-1	181	8.56	"	549